Automatic Constraint Detection for Layout Regularization

Haiyong Jiang, Liangliang Nan, Dong-Ming Yan, Weiming Dong, Xiaopeng Zhang, Peter Wonka

Abstract—In this paper, we address the problem of constraint detection for layout regularization. As layout we consider a set of two-dimensional elements where each element is represented by its bounding box. Layout regularization is important for digitizing plans or images, such as floor plans and facade images, and for the improvement of user created contents, such as architectural drawings and slide layouts. To regularize a layout, we aim to improve the input by detecting and subsequently enforcing alignment, size, and distance constraints between layout elements. Similar to previous work, we formulate the layout regularization as a quadratic programming problem. In addition, we propose a novel optimization algorithm to automatically detect constraints. In our results, we evaluate the proposed framework on a variety of input layouts from different applications, which demonstrates our method has superior performance to the state of the art.

Index Terms—layout regularization, constraint detection, constraint analysis, linear integer programming.

1 Introduction

We propose an algorithm for the regularization of layouts. In this paper, a layout refers to a two-dimensional arrangement of objects. Layouts arise in a variety of applications, for example they can come from digitized architectural floor plans, digitized facade images, image and text layouts on slides, line drawings, and graph drawings. In practice, when a layout is designed or digitized from another source (e.g., images), it is inevitable that noise occurs through imprecise user input. Elements in an idealized layout exhibit some regularities, e.g., they are aligned, of same-size, or uniformly distributed along a specific direction. However, in the aforementioned applications these regularities typically disappear due to the approximate user input. In this work, we want to detect and restore these regularities, eliminating the noise that occurred during the layout design or digitization stage.

We see three reasons why this is an important problem. First, high-level shape analysis is a popular topic in computer graphics. Many available methods rely on correctly extracted relationships to analyze a scene [1]. Even if the input and output of our regularization look visually similar, it is important that correct relationships are extracted. Our motivation for this paper, was to build datasets for machine learning techniques for layout synthesis. Second, a regularized layout compresses better than a noisy one. Therefore, regularization is important for representing layouts efficiently. Third, in most cases the visual differences are noticeable and the regularized layout looks better than the original one.

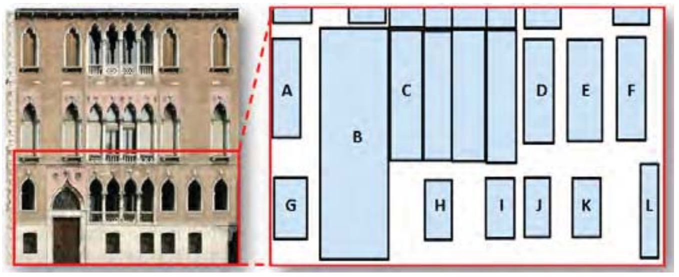

Fig. 1 Complexity and multiformity of constraints in a facade layout. Elements B and C are partially aligned (only top aligned, but not bottom aligned). The large element B is aligned with different objects at the top (C ... F) and bottom (L). Elements are missing from a regular pattern consisting of A, D, E, and F. Spacing between same-sized elements H, I, J, K is irregular.

Regularization of layouts is challenging in several ways and we discuss a few selected example challenges: 1) Elements can be partially aligned (e.g., elements are only bottom aligned, but not top aligned). 2) Large elements can be aligned with multiple objects (e.g., top aligned with one and bottom aligned with another). 3) Elements can be missing from a regular pattern. 4) Spacing between rows or/and columns can be irregular. Fig. 1 shows the complexity of possible constraints in an example layout.

A key ingredient in regularization is the design of the layout model. A simple layout model has only a few parameters and therefore the fitting process is fairly robust. These simple models, e.g., a set of regular grids, are popular for

- H. Jiang is with the National Laboratory of Pattern Recognition (NLPR), Institute of Automation, Chinese Academy of Sciences, Beijing 100190, China, and KAUST, Thuwal 23955-6900, Saudi Arabia. Email: haiyong.jiang@nlpr.ia.ac.cn.
- L. Nan is with KAUST, Thuwal 23955-6900, Saudi Arabia. Email: liangliang.nan@gmail.com
- D.-M. Yan is with KAUST, Thuwal 23955-6900, Saudi Arabia, and the National Laboratory of Pattern Recognition (NLPR), Institute of Automation, Chinese Academy of Sciences, Beijing 100190, China. Email: yandongming@gmail.com. D.-M. Yan is the corresponding author.
- W. Dong and X. Zhang are with the National Laboratory of Pattern Recognition (NLPR), Institute of Automation, Chinese Academy of Sciences, Beijing 100190, China. Email: weiming.dong@ia.ac.cn, xiaopeng.zhang@ia.ac.cn.
- P. Wonka is with KAUST, Thuwal 23955-6900, Saudi Arabia, and Arizona State University, Tempe, AZ 85287-8809. E-mail: pwonka@gmail.com.

automatic pattern analysis in images [2] and 3D shapes [3], [4]. Unfortunately, this simple data model limits the applicability to a large class of layouts, e.g., the layout shown in Fig. 1. A complex model typically has many parameters and can fit a large number of layouts. However, the model is not very robust to noise.

An initial framework for regularization was presented by Pavlidis and Van Wyk [5]. They propose a simple greedy algorithm to detect constraints from a layout. By constrast, we use an optimization approach based on four steps. First, we extract constraint candidates. Second, we score the likelihood of constraints using energy functions. Third, we use global optimization using linear integer programming to select a subset of the constraint candidates that work well together. Fourth, we regularize the layout by transforming the contents of the layout such that the change in both of the element locations and sizes is minimal while respecting the selected constraints. Our formulation of the layout regularization is an energy minimization using quadratic programming.

In our results, we will show that our algorithm has much better performance than [5] and also better performance than the independently developed algorithm in [6]. Further, our framework has more types of constraints that can be considered than previous work. The constraints we consider are constraints on the size, spacing, and alignment of layout elements.

We make the following contributions:

- We propose a formulation of the layout regularization problem that has better performance than previous work, as evaluated on a test dataset consisting of layouts from a variety of applications.
- We extend previous work by including a larger variety of constraints that can be detected and considered in the layout optimization.

2 Related Work

The layout problem can be roughly classified into two major categories, i.e., seamless layouts without gaps, and layouts with gaps between elements. Our work focuses on the latter type of layout problems. We review the most related work in image structure analysis, geometry structure analysis, and layout enhancement.

Image structure analysis. There is a large amount of structure analysis literature that addresses different aspects of image analysis and understanding. A common interest in both computer graphics and computer vision is the facade layout analysis for urban modeling [7]. The image labeling problem has been addressed by considering both visual evidence and architectural principles [8]. Based on a perceptual grouping approach, translational symmetry is exploited for single-view image recognition [9]. A similar approach that uses the repetition information for facade image reconstruction is proposed by Wu et al. [10]. To understand the structure of a facade, a set of facade images are first recursively split and labeled for training, and then the features are extracted from the segmented facades and are used to guide the labeling. Riemenschneider et al. [11] combine both low-level and mid-level classifiers for irregular facade parsing. Yang et al. [12] use a binary split grammar to parse the facade images. Teboul et al. [13] parse facade layouts by using reinforcement learning. Wu et al. [1] extract grammars from labeled facade layouts, and generate large scale variations by editing the grammars. Shen et al. [14] adaptively partition urban facades into a hierarchical structure based on concatenated and interlaced grids. Musialski et al. [15] developed an interactive tool for facade image segmentation, where a significant amount of user interaction is required. While most of these analysis of the facade layouts use a hierarchical representation, Zhang et. al. [16] proposed to model layouts using layered grids with irregular spacing. In our work, we also use grids with irregular spacing, but we can avoid the complexity of the layered structure.

Geometry structure analysis. In the 3D space, quite a few papers focus on discovering regular patterns for geometry structure analysis. Mitra et al. [17] propose a pair matching based approach to detect partial and approximate symmetry in 3D shapes. Pauly et al. [18] further introduce a framework for detecting translational, scaling and rotational patterns in 3D shapes. Tevs et al. [19] build a connection among similar shapes via geometric symmetries and regularities. These approaches have inspired many applications, such as shape analysis, reconstruction, and synthesis. For example, Li et al. [20] propose to reconstruct 3D shapes from noisy and incomplete point cloud data that simultaneously detects surface primitives and their mutual relationships. This approach involves both local and global shape analysis. We refer the reader to the recent survey paper of [21] for more related work in this topic.

Layout enhancement. The layout enhancement (regularization and beautification) has been studied in different areas, e.g., object alignment [22], handwriting and drawing beautification [23], [24], [25], sketch and drawing beautification [5], [6], [26], [27], and 3D shape symmetrization [28]. Nan et al. [29] exploit and model conjoining Gestalt rules for facade elements grouping and summarization. AlHalawani et al. [30] analysze and edit the facade images with (semi-)regular grid structures. Huang et al. [31] combine patch-based image completion and translational symmetry detection to fill the missing part of an incomplete planar structure. More recently, Xu et al. [32] propose a command-based arrangement tool for 2D layouts.

Pavlidis and Van Wyk [5] beautify drawings using a clustering method, while Xu et al. [6] interactively enhance the global beautification with user guidance. We will compare our approach to these two methods in Sec. 6.

In this work, we are interested in processing digitized 2D images and drawings. By abstracting each layout as a set of rectangles, our goal is to regularize the layout of the elements such that the regularities of the elements in the layout are enforced.

3 Overview

Given an image or drawing $\mathbf{I}$ that is characterized by a set of rectangles, the layout $L = \{e_1, ...e_n\}$ of $\mathbf{I}$ can be simply described as the locations and sizes of the elements in $\mathbf{I}$. Here, an element e_i is defined by a label l_i, and its bounding box $b_i = \{x_i, y_i, w_i, h_i\}$ depicting its bottom-left corner (x_i, y_i) and the size (w_i, h_i) (see Fig. 4). Our goal

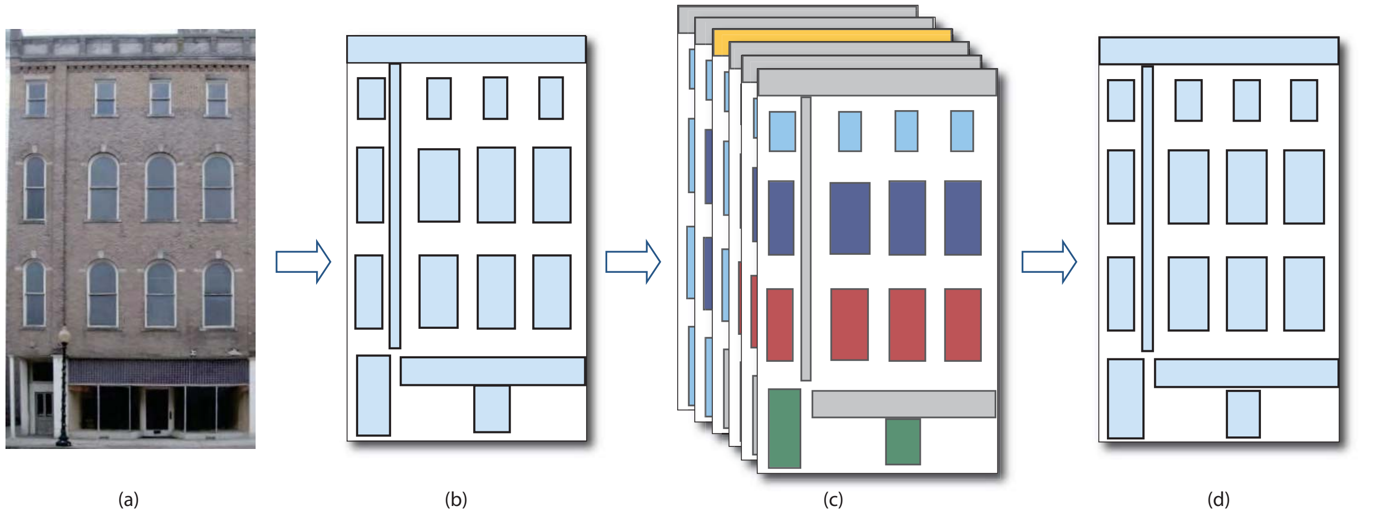

Fig. 2 An overview of our layout regularization approach. Given an input image or drawing (a), we first obtain the initial layout by manually marking and labeling the elements in a pre-processing step (b). Then appropriate constraints are automatically selected (c) and are used to generate the regularized layout (d).

is to regularize the layout of the elements such that the regularities of these elements are enforced.

Our proposed solution to the layout regularization problem uses both discrete and continuous optimization. Fig. 2 shows an overview of our layout regularization method. Our method consists of the following three steps.

Preprocessing. To digitize the layout of a given image, the user manually marks and labels the elements in the input image. The output of the preprocessing step is the initial layout that will be regularized in the next steps. Alternatively, the input can be user generated drawings or slide layouts.

Constraint selection. We first detect a larger set of candidate constraints from the initial layout using a simple thresholding based method. Then we score each constraint using an energy function. Finally, we select a set of constraints from the candidates using global optimization (linear integer programming). Details on constraint selection are described in Section 4.

Layout regularization. To regularize the input layout, we transform the contents of the layout such that the change in both of the element locations and sizes is minimal while respecting the selected constraints. We formulate the layout regularization as energy minimization using quadratic programming (Section 5).

4 Constraints Selection

Given the user marked elements in a layout, our layout regularization tries to detect and enforce three types of constraints: alignment, same-size, and same-spacing. This problem is challenging in the following ways. First, we have to detect reasonable constraints connecting elements in the layout. Second, there may exist potential conflicts among these constraints. To address these problems, we introduce an optimization-based constraint selection algorithm. The selected constraints are then used in a quadratic programming formulation to regularize the layout (see Section 5).

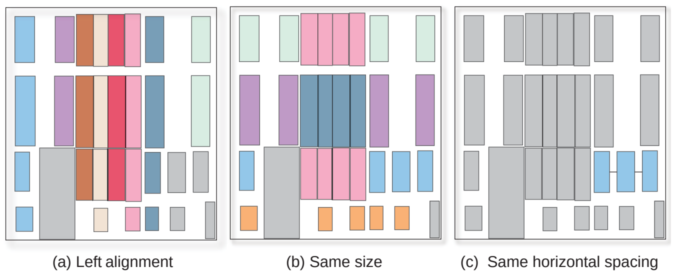

Fig. 3 A subset of constraints in the example layout in Fig. 1. Colors indicate different constraint groups in this figure.

4.1 Constraint Definitions

We consider the following relationships between elements as potential regularity constraints: alignment constraints, same-size constraints, and same-spacing constraints (see Fig. 3 and Fig. 4).

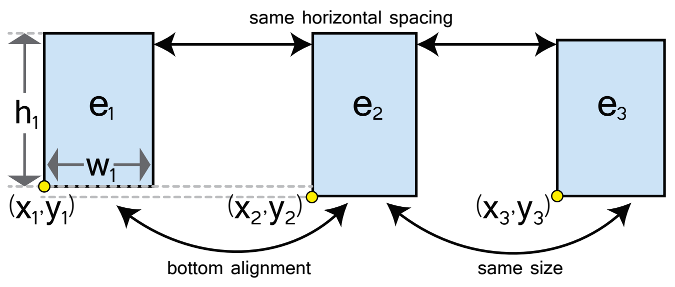

Fig. 4 Illustration of three types of constraints. The bottom alignment of element e_1 and e_2 can be formulated as $y_1 - y_2 = 0$. For the same size constraint of element pair (e_2, e_3), we have $w_2 - w_3 = 0$ and $h_2 - h_3 = 0$. The horizontal same spacing constraint on element pairs $\{e_1, e_2\}$ and $\{e_2, e_3\}$ will turn out to be $x_2 - (x_1 + w_1) - (x_3 - (x_2 + w_2)) = 0$.

Alignment constraints. Two elements e_i and e_j can have one or multiple of the following alignment constraints: top alignment, middle-Y alignment, bottom alignment, left alignment, middle-X alignment, and right alignment. For example, a bottom alignment between e_i and e_j can be formulated as

$$y_i - y_j = 0, \tag{1}$$

Other alignment relations are defined in a similar way.

Same-size constraints. Two elements e_i and e_j may be linked by a same-width constraint or a same-height constraint or both. Elements with the same label are always considered to hold both same-size constraints. Same size constraints can be formulated as:

$$\begin{aligned} w_i - w_j = 0, \\ h_i - h_j = 0. \end{aligned} \tag{2}$$

Same-spacing constraints. Same-spacing constraints are defined on $2-$element pairs and can be either in the horizontal or vertical direction. Currently, we only consider same-spacing constraints between elements with the same labels. For example, assume the element pairs (e_i, e_j) and (e_m, e_n) should have the same spacing in the horizontal direction. The equations for same-spacing constraints depend on the relative position of the elements. For the given example assuming $x_i < x_j$ and $x_m < x_n$ would lead to

$$x_i + w_i - x_j - (x_m + w_m - x_n) = 0. \tag{3}$$

4.2 Candidate Group Generation

The candidate group generation step computes a set of candidate groups $\{g_i\}$, where each group g_i is a set of elements that share an alignment, same-size, or same-spacing constraint. In this step, we use a threshold t_a to limit the candidate groups to a reasonably small set. Note that the threshold t_a is a global control mechanism for the number of candidate groups being generated. This threshold is set high enough so that all reasonable candidates are generated. Note t_a is only used for generating the candidate constraints, while the actual constraints are selected using the linear integer programming formulation described later. We describe the candidate group generation for each constraint type in the following.

Alignment constraints. We use top-alignment as an example. We sort all the elements in the input layout according to the y value of their top edge. Let $\{p_1, ...p_n\}$ denote the top positions of the sorted elements. We generate a set of potential groups, such that the difference in the top positions of every pair of the elements in each group are less than the threshold t_a.

Same-size constraints. For same size constraints, we first group all elements according to their label because we assume that elements with the same label have the same size. Then, we compute the average element size for each label and use this element size to define a distance between labels using the l_1 norm. For each label we find the k-nearest neighboring labels, where k is iterating from 1 to the number of labels. This yields an initial set of candidate groups. Then we filter out candidate groups in which there exists two elements with a size difference larger than the threshold t_a.

Same-spacing constraints. We take horizontal same-spacing as example. We sort all the element pairs in the input layout according to their horizontal intervals. Then the same-spacing constrained groups are generated by combining element pairs so that each group satisfies the following two conditions: 1) The difference in the interval of every element pair is less than the threshold t_a; 2) The elements overlap in the vertical direction.

4.3 Energy Functions

We now describe how to assign energy values to candidate groups, so groups with lower energies are more likely to be selected. We first describe a set of auxiliary heuristic functions that will then be combined to obtain various energy functions. In the optimization, we will use a linear combination of the described energy functions as the objective function. A constraint group g_i is composed of a set of elements $\{e_1, ..., e_n\}$ (2-element pairs for same-spacing). We define the following functions on g_i:

Standard deviation. The function $stdvar(g_i)$ measures the standard deviation of positions (for alignment constraints), sizes (for same-size constraints), or spacings (for same-spacing constraints). For example, if g_i is a group of top-aligned elements, $stdvar(g_i)$ is the standard deviation of the top positions of all elements in group g_i.

Maximal element distance. The function $maxDist(g_i)$ computes the maximal distance between positions, sizes, or spacings. For example, for a group of top-aligned elements, $maxDist(g_i)$ is defined as the difference between the maximal and the minimal top position in the group.

Group scale. The function $scale(g_i)$ is an intuitive measure for the scale of group g_i in the relevant direction (x or y). This function is evaluated differently for alignment, same-size, and same-spacing constraints. For example, for a group g_i with horizontal alignment, $scale(g_i)$ is equal to the minimal height of elements in group g_i. For same size constraints, $scale(g_i)$ is the maximum of the minimal width and minimal height of the elements in group g_i. For same-spacing constraints, we define $scale(g_i)$ as the minimum spacing between element pairs in g_i.

In order to measure the quality of a constraint group, we consider the following energy terms.

Intra-group distance. In our analysis, a good group should have a small variance and a small maximal element distance. Further, these values should be normalized by scale:

$$E_d(g_i) = \frac{max(0, stdvar(g_i) + maxDist(g_i) - \epsilon)}{scale(g_i)}, \tag{4}$$

where ϵ is the maximal allowed tolerance value so that distances smaller than ϵ will be ignored. We set ϵ to 3 pixels based on our experiments.

Aspect ratio variance. For same size constraints, the aspect ratio plays an important role. Thus, we use an energy term $E_a(g_i)$ that captures the standard deviation of the aspect ratio of all elements in group g_i. Here the aspect ratio of an element is defined as $\frac{w}{h}$, where w, h are the width and height of the element.

4.4 Constraint Selection

We employ linear integer programming to select a set of constraint groups among the candidate groups. There are multiple goals: First, the energy values of the selected groups should be low. Second, the complexity of the overall model measured by the number of constraint groups used should also be low. This motivates the use of an additional sparsity term. In our formulation, each constraint type uses a different energy function.

Given an input layout L consisting of n elements, and the candidate constraint groups $G = \{g_1, ..., g_N\}$ generated from L, our task is to choose a subset of these candidate groups as constraints for the following layout regularization step. Let $C = C_a \bigcup C_{ss} \bigcup C_{sp}$ denote all the constraint types, where C_a, C_{ss}, and C_{sp} are alignment, same size, and same-spacing types, respectively. $\mathbf{Z} = \{z_1, ...z_N\}$ denotes the binary label for each candidate group (1 for *chosen* and 0 for *not chosen*). We split $\mathbf{Z}$ into three subvectors $\mathbf{Z_a}$, $\mathbf{Z_{ss}}$, and $\mathbf{Z_{sp}}$ representing the labels for each type of the constraint groups. Then the energy for these types of constraint groups are defined as follows:

Alignment constraints.

$$E(\mathbf{Z_a}) = \sum_{c_j \in C_a} \sum_{g_i \in G} E_d(g_i) \cdot z_i \cdot \delta(g_i, c_j) + w_a \cdot \|\mathbf{Z_a}\|_0, \quad (5)$$

where $\|\cdot\|_0$ denotes the ℓ^0-norm, which counts the number of nonzero entries in a vector. We add this term to encourage fewer and larger groups (i.e., groups that have more elements). Since $z_i \in \{0, 1\}$ in our problem, $\|\cdot\|_0$ can be simplified to the sum of all the entries in the vector. $\delta(g_i, c_j)$ is an indicator function that has value 1 if g_i is a candidate group of constraint type c_j, otherwise zero. w_a is a weight that balances the two terms.

Same size constraints. The energy function for same size constraints is similar to that of alignment constraints. To account for aspect ratio of an element in the layout, we also involve the aspect ratio variance E_a into the formulation:

$$E(\mathbf{Z_{ss}}) = \sum_{c_j \in C_{ss}} \sum_{g_i \in G} (E_d(g_i) + w_a \cdot E_a(g_i)) \cdot z_i \cdot \delta(g_i, c_j) + w_{ss} \cdot \|\mathbf{Z_{ss}}\|_0, \quad (6)$$

Same spacing constraints. For same-spacing constraints, the energy function is similar to that of alignment constraints:

$$E(\mathbf{Z_{sp}}) = \sum_{c_j \in C_{sp}} \sum_{g_i \in G} E_d(g_i) \cdot z_i \cdot \delta(g_i, c_j) + w_{sp} \cdot \|\mathbf{Z_{sp}}\|_0, \quad (7)$$

Afterwards, proper constraint groups are selected by minimizing the following constrained objective function:

$$\begin{aligned} \underset{\mathbf{X}}{\text{minimize}} \quad & E(\mathbf{Z_a}) + E(\mathbf{Z_{ss}}) + E(\mathbf{Z_{sp}}) \\ \text{subject to} \quad & \sum_{i=1}^{N} \|g_i\| \cdot z_i \cdot \delta(g_i, c_j) = n, \quad c_j \in C \\ & z_i + z_j \leq 1, \quad \forall g_i \bigcap g_j \neq \emptyset, \quad 1 \leq i, j \leq N \\ & z_i \in \{0, 1\}, \quad 1 \leq i \leq N, \end{aligned} \quad (8)$$

where the constraints $\sum_{i=1}^{N} \|g_i\| \cdot z_i \cdot \delta(g_i, c_j) = n$ ensure that every element in the layout is assigned to a constraint group of type c_j. The second group of constraints $z_i + z_j \leq 1$ enforce that groups do not have overlapping elements if g_i and g_j are of the same constraint type.

The optimization problem above is a linear integer program that can be efficiently solved using various open source solvers, e.g., [33], [34], [35]. The solution is a set of constraint groups. Each group gives rise to a set of linear equations that serve as constraints during the layout regularization step. For example, for an alignment group $g_i = \{e_{i1}, ..., e_{iN}\}$, we combine adjacent elements to form the constraint pairs, namely, $(e_{i1}, e_{i2}), ..., (e_{i(n-1)}, e_{iN})$. Then we generate one linear equation per constraint pair.

5 Layout Regularization

With the optimal constraints detected and filtered from the constraint selection step, our final goal is to regularize the layout under these constraints. Our regularization process has a similar format with the methods of [36] and [37]. These works both emphasize on the facade structure using a hierarchical layout, while ours deals with a layout of rectangles. We address this regularization problem by transforming the contents of the layout from the input layout L to regularized layout L^* such that the change to element locations C_L and element sizes C_S is minimal while respecting the constraints. The star ($*$ in L^*) indicates the regularized layout.

To facilitate user preferences, we use a weight ω (we set as 2.5 for our preference for position changes) to balance between the two terms above. Then the layout regularization is formulated as energy minimization as below:

$$L^* = arg\min \, (C_L + \omega \cdot C_S), \quad (9)$$

where

$$C_L = \sum_{i=1}^{n} (x_i^* + \frac{w_i^*}{2} - x_i - \frac{w_i}{2})^2 + (y_i^* + \frac{h_i^*}{2} - y_i - \frac{h_i}{2})^2$$

$$C_S = \sum_{i=1}^{n} (w_i^* - w_i)^2 + (h_i^* - h_i)^2$$

In addition to the aforementioned constraints selected in Section 4, we add additional constraints to Equation 9 to ensure the validity of the optimized layout. In our formulation, we include lower bound constraints and upper bound constraints for the variables, and sequential constraints for the elements' relative positions.

- **Lower and upper bound constraints**. These constraints restrict the changes of elements in reasonable ranges. Let (w_b, h_b) denote the size of the bounding box of the layout, we add additional positional constraints $0 \leq x_i^* \leq w_b$ and $0 \leq y_i^* \leq h_b$.
  Further, to prevent the elements from being changed too much in their sizes, we also add upper bound constraints on their sizes. Let's take the width bound as an example, it is defined proportionally to the widths of all elements that have the same label ℓ. In our implementation, the maximal allowed width change for an element e_i is defined as $max(0.5 \cdot \Delta w_\ell, 0.15 \cdot w_i)$, where Δw_ℓ is the maximal difference in width for elements that have the same label, and w_i is the width of e_i. The size constraints on element height are defined similarly.
- **Sequential constraints**. These constraints specify the relative positions of pairs of elements. With these

constraints, we expect that the elements' original layout will not be greatly altered by the regularization. Our experiments show that this type of constraints is crucial to layout regularization. Given 2 X-ordered (ascending order) elements e_i and e_j, the constraints are $x_i^* + w_i^* - x_j^* \leq 0$ if $x_i + w_i - x_j \leq 0$. The same goes for the vertical direction.

By solving the quadratic programming problem defined in Equation 9, we obtain the regularized layout. In our implementation, we add the constraints sequentially in order to avoid potential conflicts. If there is any conflicts detected during the optimization, we just remove the current constraint. However, the sequence of constraints will affect the results. To incorporate our preferences for different constraints, we sort all constraints according to their energy function $stdvar(g_i)$ (see Eq. 4), and then add them to the constraint set according to this order.

6 Results and Discussion

Test database. Our experiments are conducted on a database of 32 digitized layouts from various applications. Our data set contains examples covering facades, slide designs, web designs, indoor scenes, and other graphical layouts. In Figures 5, 6, and 7 we show a set of different layouts regularized using our method. In the supplemental materials, we provide more results showing detected relations and regularized layouts. From these applications, we can see that our method enforces the regularity constraints, while preserving the high-level relations, such as symmetries and the repetitive patterns.

Evaluation metrics. In order to evaluate the effectiveness of our framework, we designed an interactive program to specify the ground truth relationships for each layout. We use the marked relations to compute precision (P), recall (R), and F-measure(F) defined as follows:

$$P = \frac{\sum\limits_{i\in G_g}\sum\limits_{j\in G_d} num(g_i \bigcap g_j)}{\sum\limits_{j\in G_d} num(g_j)},$$
$$R = \frac{\sum\limits_{i\in G_g}\sum\limits_{j\in G_d} num(g_i \bigcap g_j)}{\sum\limits_{i\in G_g} num(g_i)}, \quad (10)$$
$$F = \frac{2 \cdot P \cdot R}{P + R},$$

where G_g is the set of constraint groups in the ground truth, G_d is the set of constraint groups in the detected result, and $num(\cdot)$ is the number of constraints in a constraint group. The term $g_i \bigcap g_j$ denotes the intersection of two constraint groups. It is empty if g_i and g_j are of different types of constraints. For alignment and same size, an $n-$element constraint group will contribute $n-1$ constraint pairs, while an $n-$pair spacing group will contribute $n-1$ constraint pairs (see Section. 4.1). Thus, we define the number of constraints of a constraint group as the number of constraint pairs it yields. For example, consider we have the top alignment of elements $G = \{e_1, e_2, e_3, e_4, e_5\}$ as ground truth, but the algorithm only detects elements $D = \{e_1, e_2, e_3, e_5\}$ as top aligned. Then we have $num(D) = 4-1$, $num(G) = 5-1$, and $num(G \bigcap D) = 4-1$.

TABLE 1 Comparisons with [5] and [6] on alignment and same-spacing constraints. Our method is evaluated with and without labels. We show the average precision, recall, and F-measure for all layouts in the test dataset.

Method	Alignment			Same-spacing		
	P	R	F	P	R	F
Pav85 [5]	**0.927**	0.726	0.804	0.782	0.366	0.453
Xu2014 [6]	0.920	0.832	0.868	0.732	0.498	0.540
Ours (no label)	0.911	0.959	0.936	0.750	**0.706**	**0.710**
Ours	0.911	**0.959**	**0.936**	**0.916**	0.613	0.696

Comparison. We conducted comparisons with the methods of Xu et al. [6] and Pavlidis et al. [5]. Pavlidis et al. [5] propose to use a clustering method to detect the constraints. Xu et al. [6] empoly the RANSAC method to get alignment constraints, and a clustering method for same spacing detection. We first conduct a test of alignment constraints. Fig. 8 shows the precision, recall, and F-measure for every layout in our test database. As we can see, our algorithm has similar precision to previous work, but higher recall for most layouts. This leads to the highest F-measure results on 93.8% of layouts in the database. The comparison is also summarized in Tab. 1 left. In the next test, we compare the same-spacing constraints. In Tab. 1 right, we show the comparison of the average values for precision, recall and F-measure. From this comparison we see that the same-spacing constraint is more difficult to detect than the alignment constraint. Additionally, it was also very difficult to define a ground truth for this constraint. From the above comparison, we can see that the precision of the same spacing detection benefits from the label information. However our method still works better than others even without the label information. In Fig. 9, we also show an illustrative example of a case where our method is more successful than Xu et al. [6]. We can see that Xu et al. can not handle layouts where elements overlap with each other, thus it cannot align the elements properly. In addition, we compare the performance of these three methods by measuring the average computation time for the examples in our dataset. The method in [5] could detect the constraints in $0.001s$ because of the simplicity of the method. The method of Xu et al. [6] needs 0.898s, while ours needs about 0.914s.

Running time. We have implemented the proposed method in C++. All the experiments are performed on a PC with two 2.70GHz Intel Xeon E5-2680 processors. We found that the running time highly depends on the number of elements and the number of relations in the input layout. On average, the constraint selection step takes 0.70 seconds, and the regularization step takes 3.59 seconds. The maximum times were 3.71 seconds and 15.78 seconds, respectively.

Robustness & scalability. We evaluated the robustness and scalability of our algorithm on synthesized examples. We first generate a regular grid of elements of two different sizes with 8 columns and 5 rows. We then perturb the corners of the elements with an increasing amount of Gaussian noise (measured relative to the element sizes). The performance of our method is demonstrated in Tab. 2. We can see that

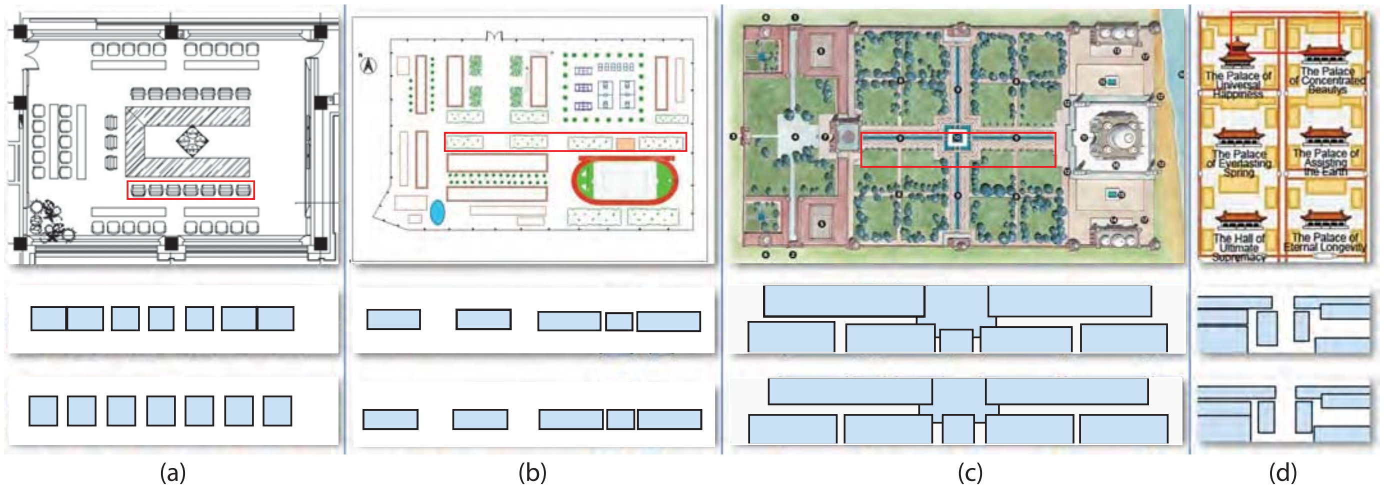
The Palace of Universal Happiness
The Palace of Concentrated Beauty
The Palace of Everlasting Spring
The Palace of Assisting the Earth
The Hall of Ultimate Supremacy
The Palace of Eternal Longevity
(a)
(b)
(c)
(d)

Fig. 5 Four different layouts are regularized using our method. Each column (from top to bottom) shows the input floor plan, zoomin of the marked region in the initial layout, and our regularized layout.

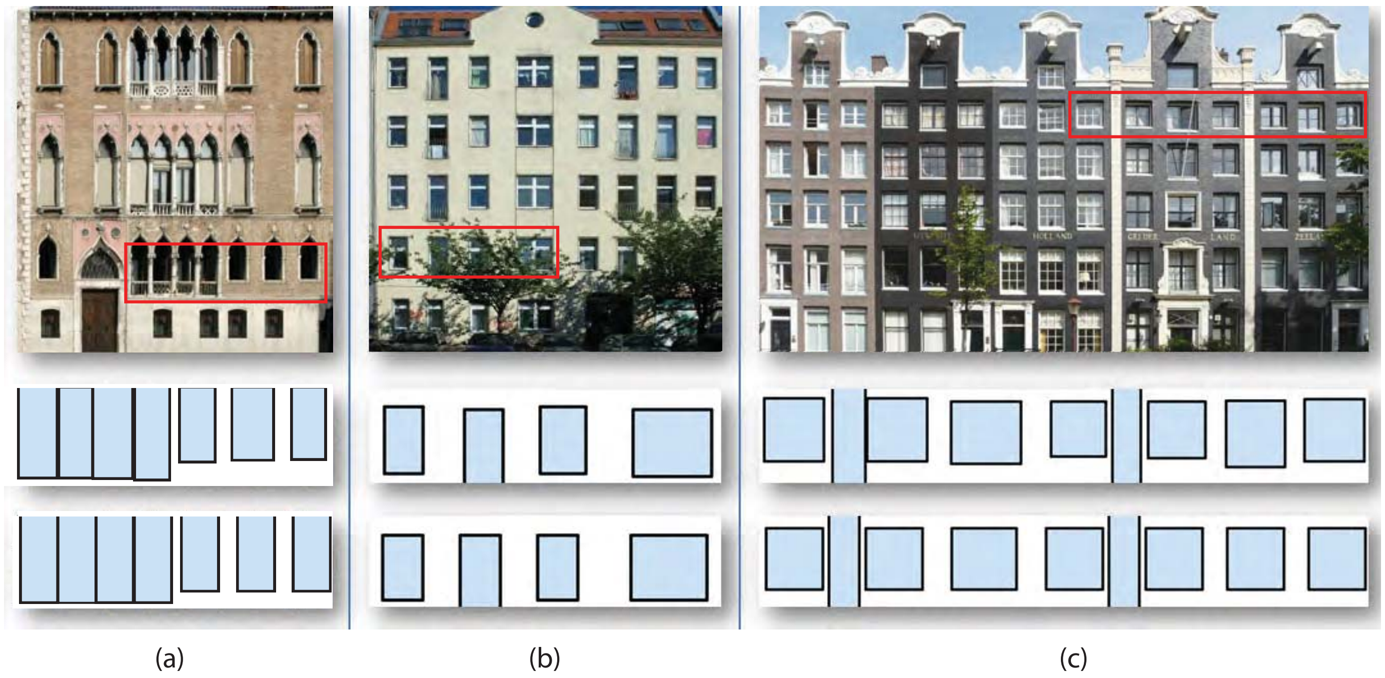

Fig. 6 Layouts regularization for a set of urban facade images. The top row shows the input facade images. The middle and the bottom rows show the zoomin views of the highlighted regions and the regularized results with abstract boxes.

our method works well if the noise is less than 10% of the element size. To evaluate the scalability, we use Gaussian noise with variance 0.02 and measure the running time for grids with a different number of elements. In Tab. 3 we show the results of this test. We can see that the accuracy decreases with larger grids. The reason is mainly that some of the same spacing constraints are not detected due to outliers.

Parameters. In our method, there exists multiple parameters. One parameter is the threshold t_a that is used to generate candidate groups. In order to verify the influence of this parameter on the results, we evaluate our method with different values of the threshold t_a on the alignment constraints (see Fig. 10). Our method can generate high quality results after a value of 0.2 times the average element size, which makes our method reliable even without user intervention. Another important parameter is the weight for

TABLE 2 Performance of our algorithm on a data set with increasing amount of Gaussian noise relative to the element size. #C is the number of detected constraints.

Level of noise	#C	P	R	F
0.00	321	1.000	1.000	1.000
0.02	321	1.000	1.000	1.000
0.04	319	1.000	0.993	0.996
0.06	297	1.000	0.915	0.956
0.08	290	1.000	0.894	0.944
0.10	263	1.000	0.795	0.886

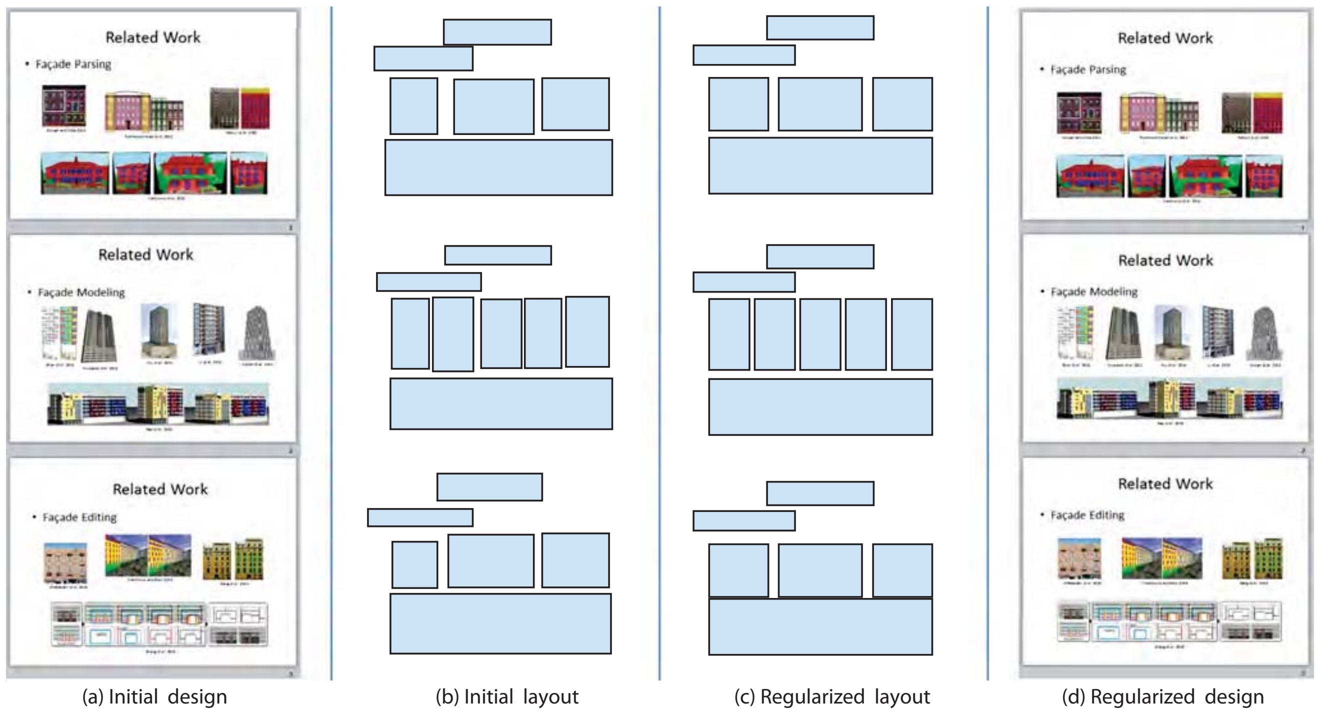

Fig. 7 Slide design beautified using our approach. From left to right: the initial design, bounding boxes of the elements in the design as input layout, optimized layout, and the final design.

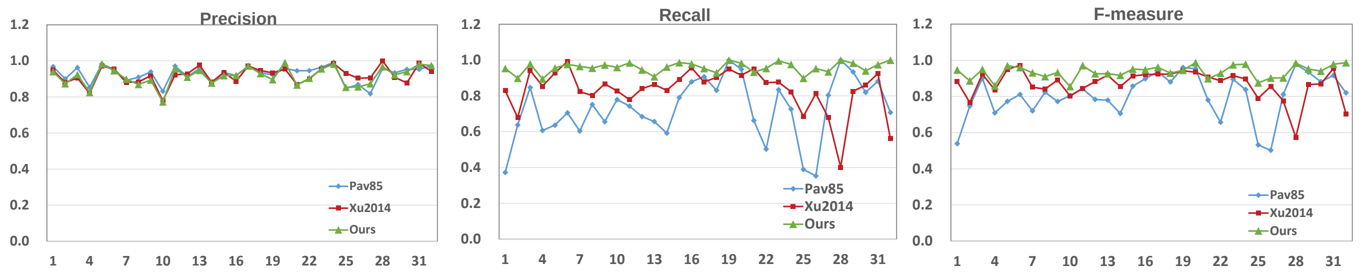

Fig. 8 The comparison of precision (left), recall (middle), and F-measure (right) of our method with Pav85 [5] and Xu2014 [6] on the alignment constraints.

TABLE 3 Performance of our algorithm on a data set with an increasing of number of rows and columns. Note that all the grid elements are perturbed by 2% Gaussian noise (relative to the element sizes).

Grid size	#C	P	R	F	Time(s)
5 × 8	321	1	1	1	2.245
10 × 8	678	0.987	0.983	0.985	6.428
5 × 16	676	0.975	0.986	0.981	6.996
10 × 16	1420	0.964	0.971	0.967	25.789
20 × 16	2940	0.947	0.964	0.955	121.822

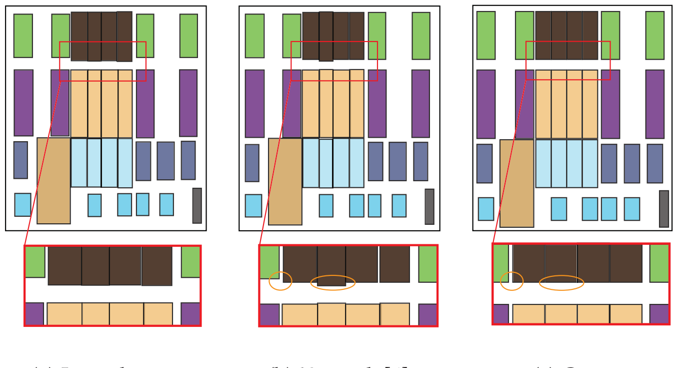

Fig. 9 A comparison of Xu et al. [6](b) and our method (c). The yellow circles indicate the differences.

the sparsity term. Here, we evaluate the performance with respect to the sparsity term w_a as shown in Fig. 11. The sparsity term plays an important role for selecting a trade off between precision and recall.

Applications. Our method is designed for general 2D layouts. One application is the regularization of digitized layouts, e.g., facade layouts shown in Fig. 6. Another application is the beautification of user drawn layouts, e.g., slide design (see Fig. 7), poster design, and other graphical

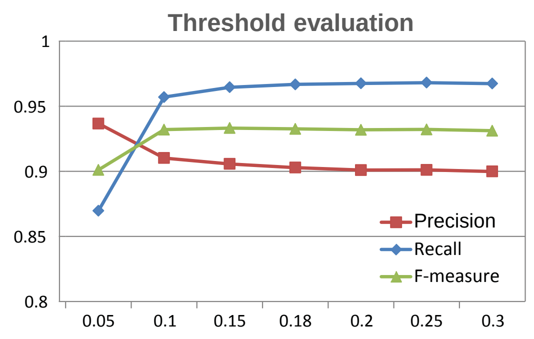

Fig. 10 The robustness of our method with respect to the threshold t_a. We show the change in average precision, recall, and F-measure for the alignment threshold uniformly sampled in the range [0.05, 0.3].

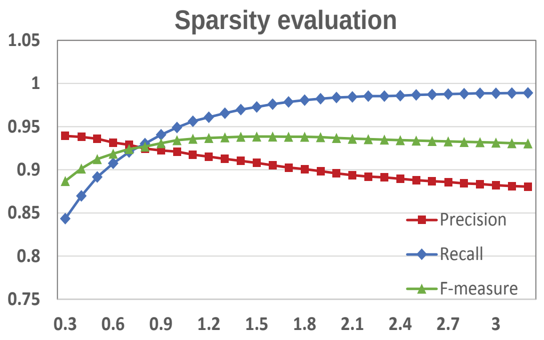

Fig. 11 The robustness of our method with respect to the sparsity term w_a.

designs (see Fig. 5).

Extensions. Our current implementation is developed for axis-aligned layouts, but we can extend our framework to consider more types of constraints and elements enclosed in oriented bounding boxes. In Fig. 12, the elements are distributed on circles. For this example, we introduce two new types of constraints that consider spacing and alignment in this radial layouts. Our algorithm can be directly used for these constraints using polar coordinate system.

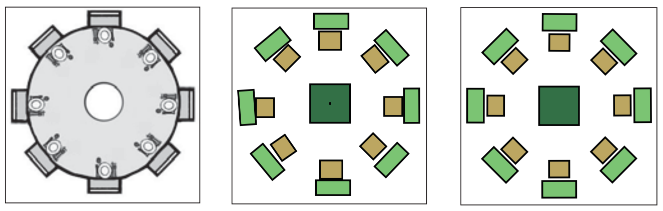

Fig. 12 An extension of our algorithm. In this example, elements (i.e., chairs or the tableware) are expected to be placed along concentric circles with same included angles. The black dot indicates the center of circles. (c) shows the result of our algorithm applied to this case by using a simple coordinate system conversion (from the Cartesian coordinate system to the polar coordinate system).

Another type of useful constraint is the same arc-length constraint. The same arc length constraint enforces a constant arc length along a curve between two adjacent points that are sampled on this curve. In Fig. 13(a), we show a set of markers (the yellow squares) that are placed along the road centerline (in the yellow color). We can see that some adjacent markers exhibit the same arc-length constraint. Directly fulfilling this constraint is difficult, considering that we do not know the curve function. We construct a map from a parameter vector to the points by a B-spline interpolation with chord length parameterization. Thus every parameter corresponds to a point, and the interval between two parameters is equivalent to the chord length of two adjacent points. Then, we achieve the same arc-length by accomplishing the same spacing constraint on the parametric vectors. In Fig. 13(c), we show the result of this regularization. Another example is demonstrated in Fig. 6 of the supplemental materials.

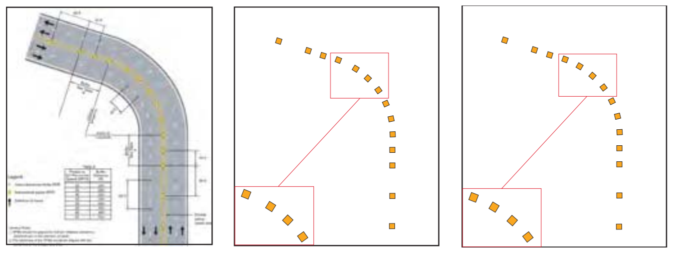

Fig. 13 The same arc-length distance constraint on points (the yellow squares). Our method successfully detects two kinds of arc length in this example and regularizes the curve points. Our framework can be applied to such input by constructing a parameterization of the points.

Our method does not fully explore the hierarchical structuring of constraints. However, we can still show such an example, where a given hierarchy defines the grouping information of elements (see Fig. 14). The regularization is achieved by applying our method from bottom to top.

Limitations and future work. Though our algorithm works well for most cases, we noticed that in some cases the result could be further improved with the availability of semantic information. For example, if there is an ornament on top of a window we can assume that there is a high probability that these two shapes are center aligned (see Fig. 15). Not using domain specific semantic priors is one limitation of our algorithm. Another limitation is that the possible constraints need to be known in advance. There is a large number of complex patterns, e.g., a set of elements being aligned along a spiral with regularly decreasing spacing, and it is unclear how our framework would perform if we would extend it using a large number of different complex constraint types. We consider this a very interesting avenue of future work. Further, we also plan to involve the user in the layout optimization stage to provide more control over the regularization process.

7 Conclusions

In this paper, we have presented an optimization-based approach for regularizing general layouts. Our method takes

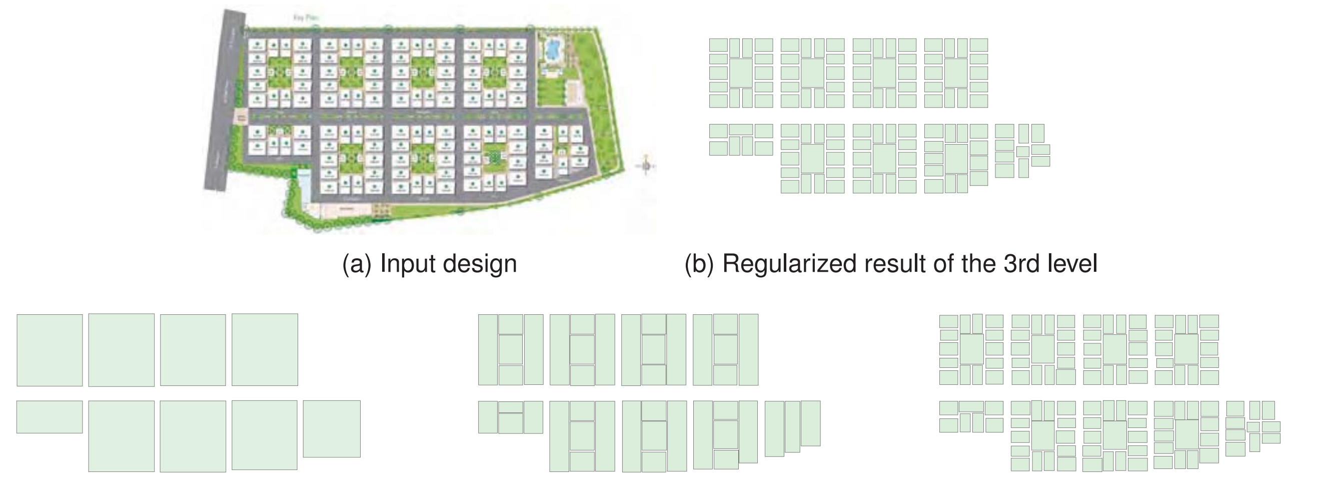

(a) Input design (b) Regularized result of the 3rd level

(c) The first level of the input layout (d) The second level of the input layout (e) The third level of the input layout

Fig. 14 The regularization of a hierarchical layout. The second row shows the hierarchy from top to down, which is marked by the user. We only use the marked hierarchy to define the group information of lower level layouts.

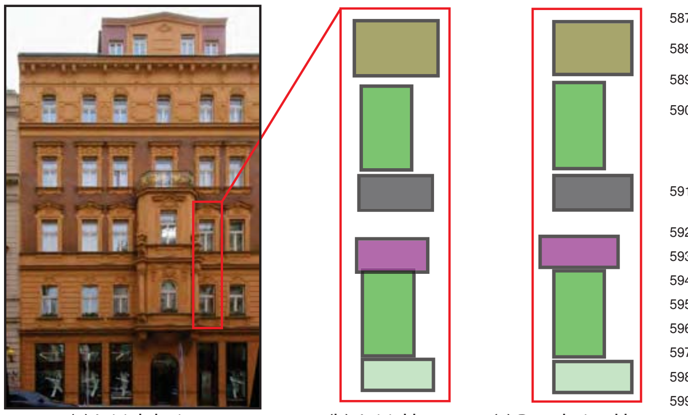

(a) Initial design (b) Initial layout (c) Regularized layout

Fig. 15 A failure case of our algorithm. In this example, the user marks a wrong left edge of the ornaments below the windows in the highlighted region due to occlusions caused by perspective projection. Semantic prior information (e.g., an ornament and window are more likely to be center aligned) is necessary to correct this error.

as input a general layout represented as a set of labeled rectangles, and detects regularity constraints based on a linear integer programming formulation. The layout is regularized by minimizing the deformation of the initial layout while respecting the detected constraints. We have evaluated our method on various input layouts. Experimental results show that our method enforces the regularities in the layout, and is superior to alternative approaches in the literature. We have also shown the usefulness of our method for various applications.

Acknowledgments

We would like to thank the reviewers for their helpful comments, and the authors of [6] for making their software public available and their help for the comparison. This work was supported by the KAUST Visual Computing Center, the National Natural Science Foundation of China (61372168, 61331018, 61271431, and 61272327), and the U.S. National Science Foundation.

References

[1] F. Wu, D.-M. Yan, W. Dong, X. Zhang, and P. Wonka, "Inverse procedural modeling of facade layouts," *ACM TOG (SIGGRAPH)*, vol. 33, no. 4, pp. 121:1–121:10, Jul. 2014.

[2] C. Wu, J.-M. Frahm, and M. Pollefeys, "Detecting large repetitive structures with salient boundaries," in *ECCV*. Springer, 2010, pp. 142–155.

[3] M. Pauly, N. J. Mitra, J. Wallner, H. Pottmann, and L. J. Guibas, "Discovering structural regularity in 3d geometry," in *ACM Transactions on Graphics (TOG)*, vol. 27, no. 3. ACM, 2008, p. 43.

[4] N. J. Mitra, A. Bronstein, and M. Bronstein, "Intrinsic regularity detection in 3d geometry," in *Computer Vision–ECCV 2010*. Springer, 2010, pp. 398–410.

[5] T. Pavlidis and C. J. Van Wyk, "An automatic beautifier for drawings and illustrations," *Computer Graphics (Proc. SIGGRAPH)*, vol. 19, no. 3, pp. 225–234, Jul. 1985.

[6] P. Xu, H. Fu, T. Igarashi, and C.-L. Tai, "Global beautification of layouts with interactive ambiguity resolution," in *UIST '14*, 2014.

[7] P. Musialski, P. Wonka, D. G. Aliaga, M. Wimmer, L. van Gool, and W. Purgathofer, "A survey of urban reconstruction," *Computer Graphics Forum*, vol. 32, no. 6, pp. 146–177, 2013.

[8] D. Dai, M. Prasad, G. Schmitt, and L. Van Gool, "Learning domain knowledge for facade labelling," in *Proceedings of the 12th European Conference on Computer Vision - Volume Part I*, ser. ECCV'12, 2012, pp. 710–723.

[9] M. Park, K. Brocklehurst, R. T. Collins, and Y. Liu, "Translation-symmetry-based perceptual grouping with applications to urban scenes," in *ACCV*, 2011, pp. 329–342.

[10] C. Wu, J.-M. Frahm, and M. Pollefeys, "Repetition-based dense single-view reconstruction," in *CVPR*, 2011, pp. 3113–3120.

[11] R. H., K. U., T. W., D. M., H. S., and B. H. Fellner D., "Irregular lattices for complex shape grammar facade parsing," in *CVPR*, 2012, p. 16401647.

[12] C. Yang, T. Han, L. Quan, and C.-L. Tai, "Parsing facade with rank-one approximation," in *CVPR*, 2012, pp. 1720–1727.

[13] O. Teboul, I. Kokkinos, L. Simon, P. Koutsourakis, and N. Paragios, "Parsing facades with shape grammars and reinforcement learning," *IEEE PAMI*, vol. 35, no. 7, pp. 1744–1756, 2013.

[14] C.-H. Shen, S.-S. Huang, H. Fu, and S.-M. Hu, "Adaptive partitioning of urban facades," *ACM Transactions on Graphics (Proceedings of ACM SIGGRAPH ASIA 2011)*, vol. 30, no. 6, pp. 184:1–184:9, 2011.

[15] P. Musialski, M. Wimmer, and P. Wonka, "Interactive coherence-based facade modeling," *Comp. Graph. Forum*, vol. 31, no. 23, pp. 661–670, May 2012.

[16] H. Zhang, K. Xu, W. Jiang, J. Lin, D. Cohen-Or, and B. Chen, "Layered analysis of irregular facades via symmetry maximization," *ACM Transactions on Graphics (Proceedings of ACM SIGGRAPH 2013)*, vol. 32, no. 4, pp. 121:1–121:10, 2013.

[17] N. J. Mitra, L. Guibas, and M. Pauly, "Partial and approximate symmetry detection for 3d geometry," *ACM Transactions on Graphics (SIGGRAPH)*, vol. 25, no. 3, pp. 560–568, 2006.

[18] M. Pauly, N. J. Mitra, J. Wallner, H. Pottmann, and L. Guibas, "Discovering structural regularity in 3D geometry," *ACM Transactions on Graphics*, vol. 27, no. 3, pp. #43, 1–11, 2008.

[19] A. Tevs, Q. Huang, M. Wand, H.-P. Seidel, and L. Guibas, "Relating shapes via geometric symmetries and regularities," *ACM TOG*, vol. 33, no. 4, pp. 119:1–119:12, Jul. 2014.

[20] Y. Li, X. Wu, Y. Chrysanthou, A. Sharf, D. Cohen-Or, and N. J. Mitra, "Globfit: Consistently fitting primitives by discovering global relations," *ACM Transactions on Graphics*, vol. 30, no. 4, pp. 52:1–52:12, 2011.

[21] N. J. Mitra, M. Wand, H. Zhang, D. Cohen-Or, and M. Bokeloh, "Structure-aware shape processing," in *EUROGRAPHICS State-of-the-art Report*, 2013.

[22] P. Baudisch, E. Cutrell, K. Hinckley, and A. Eversole, "Snap-and-go: Helping users align objects without the modality of traditional snapping," in *Proceedings of the SIGCHI Conference on Human Factors in Computing Systems*, 2005, pp. 301–310.

[23] S. Murugappan, S. Sellamani, and K. Ramani, "Towards beautification of freehand sketches using suggestions," in *Proceedings of the 6th Eurographics Symposium on Sketch-Based Interfaces and Modeling*, 2009, pp. 69–76.

[24] C. L. Zitnick, "Handwriting beautification using token means," *ACM TOG (SIGGRAPH)*, vol. 32, no. 4, pp. 53:1–53:8, Jul. 2013.

[25] P. O'Donovan, A. Agarwala, and A. Hertzmann, "Learning Layouts for Single-Page Graphic Designs," *IEEE Transactions on Visualization and Computer Graphics*, vol. 20, no. 8, pp. 1200–1213, 2014.

[26] B. Plimmer and J. Grundy, "Beautifying sketching-based design tool content: Issues and experiences," in *Proceedings of the Sixth Australasian Conference on User Interface - Volume 40*, 2005, pp. 31–38.

[27] B. Paulson and T. Hammond, "Paleosketch: Accurate primitive sketch recognition and beautification," in *Proceedings of the 13th International Conference on Intelligent User Interfaces*, 2008, pp. 1–10.

[28] N. J. Mitra, L. Guibas, and M. Pauly, "Symmetrization," *ACM TOG (SIGGRAPH)*, vol. 26, no. 3, pp. 63:1–63:8, 2007.

[29] L. Nan, A. Sharf, K. Xie, T.-T. Wong, O. Deussen, D. Cohen-Or, and B. Chen, "Conjoining gestalt rules for abstraction of architectural drawings," *ACM TOG (SIGGRAPH Asia)*, vol. 31, no. 6, p. 185:1185:10, 2012.

[30] S. AlHalawani, Y.-L. Yang, H. Liu, and N. J. Mitra, "Interactive facades: Analysis and synthesis of semi-regular facades," *Computer Graphics Forum (Eurographics)*, vol. 32, no. 22, pp. 215–224, 2013.

[31] J.-B. Huang, S. B. Kang, N. Ahuja, , and J. Kopf, "Image completion using planar structure guidance," vol. 33, no. 4, p. to appear, 2014.

[32] P. Xu, H. Fu, C.-L. Tai, and T. Igarashi, "GACA: Group-aware command-based arrangement of graphic elements," in *Proceedings of the 33rd Annual ACM Conference on Human Factors in Computing Systems*, ser. CHI '15, 2015, pp. 2787–2795.

[33] Lpsolve, http://lpsolve.sourceforge.net/.

[34] CBC, https://projects.coin-or.org/Cbc.

[35] GLPK, http://www.gnu.org/software/glpk/.

[36] M. Dang, D. Ceylan, B. Neubert, and M. Pauly, "Safe: Structure-aware facade editing," vol. 33, no. 2, pp. 83–93, 2014.

[37] F. Bao, M. Schwarz, and P. Wonka, "Procedural facade variations from a single layout," *ACM Trans. Graph.*, vol. 32, no. 1, pp. 8:1–8:13, 2013.

Haiyong Jiang is a Ph.D. student at the National Laboratory of Pattern Recognition of the Institute of Automation, Chinese Academy of Sciences (CAS). He received his Bachelor's degrees from University of Science and Technology Beijing in 2012. His research interests lie in computer graphics and computer vision.

Liangliang Nan received his bachelor's degree from Nanjing University of Aeronautics and Astronautics (NUAA), in 2003 and the Ph.D. degree from Shenyang Institute of Automation (SIA), Chinese Academy of Sciences in 2009. He currently works as a research scientist at King Abdullah University of Science and Technology (KAUST). His research interests lie in the fields of computer graphics, computer vision, and human-computer interaction.

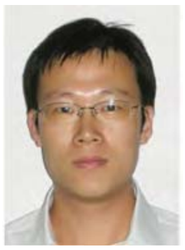

Dong-Ming Yan is a research scientist at King Abdullah University of Science and Technology (KAUST), and he is an associate professor at the National Laboratory of Pattern Recognition of the Institute of Automation, Chinese Academy of Sciences (CAS). He received his Ph.D. from Hong Kong University in 2010 and his Master's and Bachelor's degrees from Tsinghua University in 2005 and 2002, respectively. His research interests include computer graphics, geometric processing and visualization.

Weiming Dong is an associate professor in the Sino-French Laboratory (LIAMA) and National Laboratory of Pattern Recognition (NLPR) at Institute of Automation, Chinese Academy of Sciences. He received his BSc and MSc degrees in computer science in 2001 and 2004, both from Tsinghua University, P. R. China. He received his PhD in computer science from the University of Henri Poincaré Nancy 1, France, in 2007. His research interests include image synthesis and image analysis. Weiming Dong is a member of ACM and IEEE.

Xiaopeng Zhang is a professor at the National Laboratory of Pattern Recognition of the Institute of Automation, Chinese Academy of Sciences (CAS). He received his Ph.D. degree in Computer Science from the Institute of Software, CAS in 1999. He received the National Scientific and Technological Progress Prize (second class) in 2004. His main research interests include computer graphics and image processing.

Peter Wonka received his Ph.D. degree in computer science and M.S. degree in urban planning from the Technical University of Vienna, Vienna, Austria, in 2001 and 2002, respectively. He was a postdoctoral researcher with the Georgia Institute of Technology, Atlanta, GA, USA, for two years. He is currently a professor with the Computer, Electrical and Mathematical Sciences and Engineering Division, King Abdullah University of Science and Technology, Thuwal, Saudi Arabia, and also an associate professor with Arizona State University, Tempe, USA. His research interests include topics in computer graphics, visualization, computer vision, remote sensing, image processing, and machine learning.